HHS Public Access

Author manuscript

Ann Surg Oncol. Author manuscript; available in PMC 2023 February 23.

Published in final edited form as:

Ann Surg Oncol. 2022 November ; 29(12): 7781–7788. doi:10.1245/s10434-022-12157-0.

Multidimensional Immunophenotyping of Intraductal Papillary Mucinous Neoplasms Reveals Novel T Cell and Macrophage Signature

Austin M. Eckhoff, MD[1], **Ashley A. Fletcher, MS**[1], **Karenia Landa, MD**[1], **Matthew Iyer, MD PhD**[1], **Daniel P. Nussbaum, MD**[1], **Chanjuan Shi, MD PhD**[2], **Smita K. Nair, PhD**[1], **Peter J. Allen, MD**[1]

[1]Department of Surgery, Duke University; Durham, North Carolina, USA.

[2]Department of Pathology, Duke University; Durham, North Carolina, USA.

Abstract

Background: Intraductal papillary mucinous neoplasms (IPMN) are the main radiographically identifiable precursor to pancreatic adenocarcinoma, yet little is known about how these lesions progress to cancer. Inflammation has been found to be associated with progression, however the cause and composition of this inflammation remains poorly characterized. We sought to comprehensively profile immune cell tissue infiltration using parallel spatial transcriptomic and flow cytometric techniques.

Methods: Twelve patients with resected IPMN exhibiting both high-grade dysplasia (HGD) and low-grade dysplasia (LGD) were selected for spatial transcriptomics (NanoString GeoMx). Immune ($CD45^+$), epithelial ($PanCK^+$), and stromal (SMA^+) compartments were analyzed separately using the GeoMx NGS Pipeline. An additional 11 patients resected for IPMN of varying degrees of dysplasia underwent immunophenotyping using flow cytometry (DURAClone IM).

Results: Spatial transcriptomic profiling identified T cells as the dominant CD45+ cell within IPMN stroma (56%). This finding was confirmed by flow cytometry (T cells: 55%, IQR 45-68%). Spatial profiling of stromal regions immediately adjacent to the ductal epithelium identified the T cell infiltrate to be significantly higher in regions of LGD compared to HGD (62% vs 50%, p = 0.038). Macrophages were the only other immune cell type with >10% abundance, yet conversely, were more abundant in regions of HGD compared to LGD (19% vs. 11%, p = 0.058). Correspondingly, CD45+ cells in HGD demonstrated transcriptional upregulation of genes associated with macrophage activity, including secretion (CXCL1) and phagocytosis (C1QA, C4B, FGCR2A/B). All other immune cell types were infrequently seen and were not differentially abundant between HGD versus LGD stroma.

Conclusion: The leukocyte infiltrate in IPMN is primarily composed of T cells and macrophages. Regions of HGD appear to be enriched for macrophages and relatively deplete

*Corresponding Author: Peter J. Allen MD, DUMC MSRB1, Room 475, 203 Research Drive, Durham, NC 27710, peter.allen@duke.edu, Phone: 919-613-1474.

Financial Disclosures: None

of T cells compared to regions of LGD. These findings are supported by a transcriptional signature of pro-inflammatory macrophage activity in regions of HGD.

Introduction

Intraductal papillary mucinous neoplasms (IPMN) are cystic lesions of the pancreatic ductal epithelium that show varying degrees of cellular atypia and have the potential to progress to pancreatic cancer.[1] These lesions occur in up to 10% of patients over 70 years of age, and although the minority will progress, it is presumed this pathway accounts for 15 −20% of all pancreatic cancer (PDAC) cases.[2,3] Management is challenging, as we currently have limited ability to determine the level of epithelial dysplasia without operation, and are unable to predict either the timing or location of malignant progression.[4] Understanding which IPMN progress to cancer, and the mechanism of oncogenesis, may provide valuable insight that could identify opportunities for prevention and/or interception.

Previous work by our group, and others, has found inflammation to be associated with malignant progression. In 2011, Reid et al. identified tumor infiltrating neutrophils to be associated with the epithelium of high-grade dysplasia compared to low-grade dysplasia.[5] This finding has been confirmed by others, and we have utilized this finding as an approach to biomarker development in IPMN by associating cyst fluid inflammatory markers with high-grade dysplasia. [4,6,7]

Because of the heterogeneity of dysplasia, as well as the challenges of single-cell approaches in the pancreas, bulk tissue analyses have not been able to clearly define the specifics of the immune cell infiltrate in IPMN. We hypothesized that there is an immune signature within the tumor microenvironment corresponding to the degree of dysplasia. In this study, we perform spatial transcriptomic profiling of IPMN with a focus grade of dysplasia and comprehensively profile immune cell infiltration within IPMN using parallel spatial transcriptomic and flow cytometric techniques.

Materials and Methods

Patient Recruitment

All work was performed using Institutional Review Board (IRB) approved protocols. For the spatial transcriptomic analysis, Duke University Health System (DUHS) pathology archives were searched for IPMN lesions from 2017-2021 and archived hematoxylin and eosin (H&E) stained sections were reviewed by a board-certified pathologist specializing in pancreatic pathology to confirm diagnoses (CS). Slides were reviewed, and were only included if regions of LGD and HGD could be identified within a single H&E slide, and thus could serve as their own internal control.

Identification of patients for flow cytometry was done in a prospective manner. Eligible patients were 18 years or older with a presumed diagnosis of IPMN who were proceeding to standard of care surgical resection at DUHS between December 2018 and January 2022. Patients consented to research blood and tumor tissue collection prior to operation through the Duke BioRepository and Precision Pathology Center (BRPC) at Duke University School

of Medicine. De-identified tumor tissue from consented patients was obtained by BRPC and used for examination of the cellular immunome.

For both analyses, clinicopathological data was collected by study coordinators and securely stored in a RedCap database.

Spatial Transcriptomics

The NanoString GeoMx Digital Spatial Profiler (DSP) enables spatially resolved RNA gene expression. Detailed methods have previously been described.[8] For this experiment, 5 μm thick serial sections derived from FFPE tissue blocks were cut. One section was stained with H&E and one unstained section was mounted on a positively charged histology slide for use in the DSP. Whole slide imaging of the H&E sections was performed on a Nikon TE2000-E microscope.

Regions of interest (ROIs) were selected by a board-certified pathologist that featured either LGD or HGD epithelial components and adjacent stroma. Additionally, the pathologist annotated the histology subtype (gastric, intestinal, pancreaticobiliary) for each ROI. We utilized three fluorescently conjugated antibodies (morphology markers) as a means separate the ROIs into our cell populations of interest and perform segmental analysis: CD45 for immune cells, smooth muscle actin (SMA) for stroma fibroblast, anti-pan-cytokeratin (panCK) for epithelial cells. DSP tissue slides were incubated with the fluorescently conjugated antibodies to CD45, panCK, and SMA along with a cocktail of photo-cleavable-oligo-labeled primary antibodies from the GeoMX Cancer Transcriptome Atlas kit (approx. 1800 genes). See Figure 1.

Slides were loaded onto a DSP instrument and a programmable digital micromirror device directed UV light to precisely illuminate the ROI and cleave photo-cleavable-oligo-labeled primary antibodies in a region-specific manner. The released indexing oligos were then collected via microcapillary aspiration and dispensed into a microplate.[8,9] Libraries were built according to the NanoString GeoMx Library Prep Manual and pooled to equimolar concentration. RNA was sequenced under standard conditions on a Novaseq6000 to a depth of 30 read-pairs/um$^{2.}$

Next-generation sequencing quality control parameters were set to remove segments with less than 1000 raw reads, less than 80% raw read alignment, negative probe count geomean less than 4, and minimum nuclei less than 20. Biological probe QC was performed and a high confidence detection threshold was set at two standard deviations above the geometric mean of the negative probes. For the CD45 segment, 8151 out of 8659 genes (94.1%) in the full panel were above the detection threshold in at least one ROI. The 508 genes below the detection threshold in all ROIs were excluded from further CD45 analysis. A total of 48 ROIs containing CD45+ cells within the stroma were selected. Adequate hybridization and immune gene-expression profiles were generated for 25 ROIs.

Flow Cytometry

Resected tumors were collected and stored in MACS tissue storage solution at 4°C (Miltenyi). Storage time was 1–16 h post-tumor collection. Tumor tissue was mechanically

disrupted with scissors until tumor pieces were 1-2mm. Tissue was then digested in RPMI with 10% FBS 10mM Hepes 5MM CaCl2 1x protease inhibitor cocktail 1x trypsin inhibitor 100U per ml DNase. Tissue and digestion media was heated to 37C for 20-40 minutes until homogenization was achieved. Tumor cells were filtered two times using a 70μM cell strainer to remove dead cell debris and resuspended in 1ml of PBS. This single cell suspension was immediately analyzed by flow cytometry.

All analyses were performed using DuraClone IM (Immune Monitoring) basic panel (CD45, CD3, CD4, CD8, CD19, CD14, CD16, CD56). Tumor was digested as above and 1×10^6 cells were added to the basic panel tube and cells were processed according to the manufacturer's instructions. In brief, cells were incubated with the antibodies for 15 min in the dark. Cells were then washed twice in PBS prior to data acquisition and propidium iodide was added as a live/dead marker. Processed samples were then analyzed on a 13-color CytoFlex flow cytometer (Beckman Coulter). Data was analyzed using Kaluza Software (Beckman Coulter).

Statistical Analysis

For the spatial transcriptomic analysis, probe count data was obtained and differential expression (DE) analysis was performed using the GeoMx DSP Analysis Suite software. Analysis of DE using a linear mixed-effects model statistical test was used to compare gene expression between LGD and HGD lesions and between intestinal and pancreatobiliary subtype lesions.

NanoString SpatialDecon is a validated algorithm for quantifying cell populations by using canonical gene expression from single cell sequencing within various human tissues. NanoString has complied cell profile matrices for 75 tissue types using single cell gene expression.[10] To determine the immune infiltrate within the IPMN stroma, we employed the SafeTME matrix from SpatialDecon which is a cell profile matrix that combines cell profiles derived from flow-sorted PBMCs, scRNA-seq of tumors, and RNA-seq of flow sorted stromal cells and has been specifically designed to profile the immune and stromal cell types found in tumors.[10,11]

Flow cytometry analysis was performed in Prism and a Mann-Whitney test was used to compare cell populations between LGD and HGD lesions.

Results

Patient Characteristics

Spatial transcriptomic analysis was performed on 12 patients who had been resected for IPMN at DUHS between 2017 and 2021. These 12 patients had tumor heterogeneity characteristic for IPMN with regions of LGD and HGD within the same slide. Basic patient demographics and clinical characteristics can be seen in Table 1. The majority of patients had either main-duct (42%) or mixed-type (33%) IPMN. High-grade regions were balanced between pancreatobiliary (50%) and intestinal (50%) sub-type. Pancreatic cancer was present in four of twelve patients (33%). Within this group, two patients had an AJCC stage IA cancer and two patients had stage IIA cancer.

Identification of patients for flow cytometry was done in a prospective manner, and a total of 11 patients between December 2018 and January 2022 were identified who underwent pancreatic resection for presumed IPMN. With the exception of two patients, these patients were unique from the spatial transcriptomics cohort. Grade of dysplasia was determined as the highest grade of dysplasia seen upon histological review. For example, a patient with an LGD background and a foci of HGD was categorized as HGD. Within the flow cytometry group, three patients had IPMN with low grade dysplasia and eight patients had IPMN with high grade IPMN or invasive cancer. Basic patient demographics can be seen in Table 1 and are similar to the patient demographics from our spatial transcriptomics cohort.

IPMN Tissue Immune Infiltrate is Predominantly T Cells

Adequate hybridization and immune gene-expression profiles were generated for 25 ROIs (12 corresponding to LGD surrounding stroma, 13 corresponding to HGD surrounding stroma). First, we were interested in if there was a difference in the total immune infiltrate (CD45+ cells) between LGD and HGD. Since each region of interest has a slightly different shape and area, we normalized the total CD45+ cells within each ROI to mm squared. There was no difference in the total immune cell infiltration/mm^2 between LGD and HGD (3.11 vs 4.35 cells/mm^2 $p = 0.57$) (Figure 2a). Because there was no difference in total immune cell infiltration/ mm^2, we compared abundance scores to analyze the immune cell subtypes present within the stroma. We identified T cells to be the dominant immune cell within the IPMN stroma and that T cell infiltrate was significantly higher in regions of LGD compared to HGD (62% vs 50%, $p = 0.038$). Macrophages were the only other immune cell type with >10% abundance, yet conversely, were more abundant in regions of HGD compared to LGD (19% vs 11%, $p = 0.058$, Figure 2b). All other immune cell types were infrequently seen (<10%) and were not differentially abundant between HGD versus LGD stroma. There was no difference in CD4+ naïve T cells, CD4+ memory T cells, CD8+ naïve T cells, CD8+ memory T cells, and T regulatory cells between LGD and HGD. Although not significant, there were no T regulatory cells seen within LGD. (Figure 2c).

Differential Gene Expression between Immune Cell Populations

Differential gene expression analysis between LGD and HGD within the CD45+ segments identified transcriptional upregulation of genes associated with macrophage secretion (CXCL1) and complement genes (C1QA, C1QB, C4B) involved in macrophage phagocytosis. Additionally, we see upregulation of CD74 in HGD which is a receptor for the cytokine macrophage migration inhibitory factor and regulates cell survival and proliferation (Figure 2d).[12]

Histological Subtype

Within the 25 ROIs that passed QC, eight were pancreatobiliary, nine were intestinal, and eight were gastric. We examined the immune infiltration in IPMN lesions that were pancreatobiliary vs intestinal and found a trend towards intestinal lesions having greater total T cell abundance (intestinal, 58% vs pancreatobiliary, 47%; $p = 0.074$). Additionally, we identified 58 genes with 1.5 fold change DE between intestinal and pancreatobiliary subtype. Multiple of the genes upregulated in intestinal type IPMN are implicated in MHC I antigen presentation and T cell activity (Figure 3).

Flow Cytometry Validation

The gating strategy for analyzing CD45+ cells within IPMN tissue is presented in Supplementary Figure 1. Data were collected from a total of 11 patients, 3 of whom had LGD and 8 of whom had HGD. Overall, CD3+ T cells accounted for the majority of infiltrating lymphocytes which mirrors our spatial transcriptomic findings (55%, IQR 45-68%). Although not statistically significant, we found that the LGD IPMN stroma was enriched for total T cells and that HGD IPMN stroma was relatively deplete (LGD 71% vs. HGD 50% p = 0.085, Figure 2e).

Discussion

Pancreatic cancer is a stroma-rich cancer, and thus the tumor microenvironment has been hypothesized to be of particular importance.[13] Until recently, attempts to spatially resolute the tumor microenvironment in IPMN were limited to histopathology and immunohistochemistry (IHC). These early studies suggested a prognostic role of tumor associated neutrophils but did not characterize the role of other immune components in the progression from LGD to HGD IPMN.[5,6] In this study, we describe a spatial transcriptomics approach to profiling the tumor microenvironment of IPMN with the goal of understanding the immune components that delineate lesions with aggressive potential. We found that T cells were the predominant immune infiltrate within the IPMN stroma, and that T cells were differentially abundant in LGD vs HGD lesions. Additionally, we found that macrophages were the second most common tumor infiltrating immune cell and that macrophages were present in greater numbers in HGD lesions compared to LGD lesions. Flow cytometric analysis further validated the finding of T cells being the predominant CD45+ cell within the stroma of IPMN.

Recently, a few studies have attempted to elucidate the role of the tumor immune microenvironment in the dysplastic progression of IPMN. Notably, Bernard et al isolated IPMN stromal cells and used single cell RNA sequencing to identify the immune infiltrate within LGD IPMN, HGD IPMN, and PDAC tumors. Bernard et al found that LGD IPMNs had a pro-inflammatory immune infiltration composed of activated T cell subsets in contrast to the tumor microenvironment of HGD and invasion lesions which was enriched for myeloid-derived suppressor cells. However, they noted that with progression to LGD to invasive cancer, there was heterogenous alterations within the tumor microenvironment and that LGD IPMN harbored subsets of single cells with a transcriptomic profile that overlapped invasive cancer. [14] Distinctive to IPMN is tumor dysplastic heterogeneity with different grades of dysplasia and histological subtypes coexisting within the same lesion. In our slides, we have noted that regions of HGD and LGD dysplasia may be less than 0.5mm apart. Thus, the overlapping transcriptomic profile seen in Bernard et al's work may be due to the fact that the IPMN lesions were not micro-dissected and most likely contained heterogenous dysplasia. A strength of our current study is the isolation and spatial resolution of true HGD and LGD within a heterogenous tumor in addition to the graded dysplasia allowing each patient to serve as their own control for gene expression.

Prior literature has suggested that the tumor microenvironment in PDAC is T cell deplete due to inhibition by myeloid-derived suppressor cells and have even correlated T cell

abundance with PDAC survival.[15-18] To better understand the role of T cells within IPMN, Roth et al employed multiplex IHC to profile T cell stroma infiltration and showed that regions of LGD contained diverse T cell subtypes including cytotoxic CD8+ T cells. This immune infiltrate diversity was was progressively lost during dysplastic progression and invasive PDAC was dominated by that regulatory T cells.[19] Although we did not see a statistical difference in T cell subpopulations between LGD and HGD, regulatory T cells were present in HGD, but not in LGD, suggestive of an immunosuppressive environment.

Unique to our study is the examination of the difference in immune infiltration between the pancreatobiliary and intestinal histological subtypes of IPMNs. We noted a trend towards greater T cell enrichment in the intestinal subtype compared to the pancreatobiliary subtype and differential gene expression in T cell and MHC I signal pathways between the subtypes. Further work is needed to fully investigate whether there is a difference in the local immune response to pancreatobiliary vs intestinal IPMN subtypes.

Although spatial transcriptomics provides new tools for high resolution spatial profiling of tissue, it is not without its limitations. Currently, spatial transcriptomics does not achieve single-cell resolution and we are not able examine the cell-to-cell proximity with our data. Other limitations of this study are both its small patient sample size and the relatively low number of ROIs that passed QC. The tissue from 12 patients with IPMN was analyzed with spatial transcriptomics and out of our 48 ROIs, only 25 (52%) of those passed QC and were used for analysis. In contrast, 86% of our epithelial regions passed QC. Our lab has been investigating why so few of our ROIs passed QC and believe it be partly attributed to the low cell density within the stroma and the NanoString DSP’s systems dependence on having at least 20 cells per ROI. We have plans for stringent QC prior to future spatial transcriptomics and newer spatial transcriptomics technologies are in development to provide single cell resolution which would allow for detecting gene expression in low density cell populations.

In conclusion, we present the first reported spatial transcriptomics profiling of IPMN lesions and provide strong evidence that the IPMN immune infiltrate is primarily composed of T cells and macrophages. We noted that regions of HGD appear to be enriched for macrophages and relatively deplete of T cells compared to regions of LGD. Further studies are needed to understand how the relationship between T cells and macrophages drives malignant progression in IPMN. However, we believe that spatial transcriptomics is the optimal method for profiling the tumor microenvironment in IPMN given its unbiased approach and ability to account for tumor dysplastic heterogeneity.

Supplementary Material

Refer to Web version on PubMed Central for supplementary material.

Acknowledgements:

Austin Eckhoff acknowledges support by a NIH T-32 Grant (T32-CA093245) for translational research in surgical oncology and from the Duke Cancer Institute as part of the P30 Cancer Center Support Grant (Grant ID: P30 CA014236).

References:

1. Walsh RM, Perlmutter BC, Adsay V, et al. Advances in the management of pancreatic cystic neoplasms. Curr Probl Surg. Jun 2021;58(6):100879. [PubMed: 34144739]
2. Attiyeh MA, Fernández-Del Castillo C, Al Efishat M, et al. Development and Validation of a Multi-institutional Preoperative Nomogram for Predicting Grade of Dysplasia in Intraductal Papillary Mucinous Neoplasms (IPMNs) of the Pancreas: A Report from The Pancreatic Surgery Consortium. Ann Surg. Jan 2018;267(1):157–163. [PubMed: 28079542]
3. de Jong K, Nio CY, Hermans JJ, et al. High prevalence of pancreatic cysts detected by screening magnetic resonance imaging examinations. Clin Gastroenterol Hepatol. Sep 2010;8(9):806–811. [PubMed: 20621679]
4. Maker AV, Katabi N, Qin L-X, et al. Cyst fluid interleukin-1beta (IL1beta) levels predict the risk of carcinoma in intraductal papillary mucinous neoplasms of the pancreas. Clinical cancer research : an official journal of the American Association for Cancer Research. 2011;17(6):1502–1508. [PubMed: 21266527]
5. Reid MD, Basturk O, Thirabanjasak D, et al. Tumor-infiltrating neutrophils in pancreatic neoplasia. Modern Pathology. 2011/12/01 2011;24(12):1612–1619. [PubMed: 21822201]
6. Sadot E, Basturk O, Klimstra DS, et al. Tumor-associated Neutrophils and Malignant Progression in Intraductal Papillary Mucinous Neoplasms: An Opportunity for Identification of High-risk Disease. Annals of Surgery. 2015;262(6):1102–1107. [PubMed: 25563865]
7. Gaiser RA, Pessia A, Ateeb Z, et al. Integrated targeted metabolomic and lipidomic analysis: A novel approach to classifying early cystic precursors to invasive pancreatic cancer. Sci Rep. 2019;9(1):10208–10208. [PubMed: 31308419]
8. Beechem JM. High-Plex Spatially Resolved RNA and Protein Detection Using Digital Spatial Profiling: A Technology Designed for Immuno-oncology Biomarker Discovery and Translational Research. Methods Mol Biol. 2020;2055:563–583. [PubMed: 31502169]
9. Merritt CR, Ong GT, Church SE, et al. Multiplex digital spatial profiling of proteins and RNA in fixed tissue. Nature Biotechnology. 2020/05/01 2020;38(5):586–599.
10. Danaher P, Kim Y, Nelson B, et al. Advances in mixed cell deconvolution enable quantification of cell types in spatial transcriptomic data. Nature Communications. 2022/01/19 2022;13(1):385.
11. Han X, Zhou Z, Fei L, et al. Construction of a human cell landscape at single-cell level. Nature. 2020/05/01 2020;581(7808):303–309. [PubMed: 32214235]
12. Gil-Yarom N, Radomir L, Sever L, et al. CD74 is a novel transcription regulator. Proceedings of the National Academy of Sciences. 2017;114(3):562–567.
13. Chang JH, Jiang Y, Pillarisetty VG. Role of immune cells in pancreatic cancer from bench to clinical application: An updated review. Medicine (Baltimore). Dec 2016;95(49):e5541. [PubMed: 27930550]
14. Bernard V, Semaan A, Huang J, et al. Single-Cell Transcriptomics of Pancreatic Cancer Precursors Demonstrates Epithelial and Microenvironmental Heterogeneity as an Early Event in Neoplastic Progression. Clin Cancer Res. Apr 1 2019;25(7):2194–2205. [PubMed: 30385653]
15. Balachandran VP, Łuksza M, Zhao JN, et al. Identification of unique neoantigen qualities in long-term survivors of pancreatic cancer. Nature. 2017/11/01 2017;551(7681):512–516. [PubMed: 29132146]
16. Yang S, Liu Q, Liao Q. Tumor-Associated Macrophages in Pancreatic Ductal Adenocarcinoma: Origin, Polarization, Function, and Reprogramming. Frontiers in cell and developmental biology. 2021;8:607209–607209. [PubMed: 33505964]
17. Kemp SB, Pasca di Magliano M, Crawford HC. Myeloid Cell Mediated Immune Suppression in Pancreatic Cancer. Cell Mol Gastroenterol Hepatol. 2021;12(5):1531–1542. [PubMed: 34303882]
18. Clark CE, Hingorani SR, Mick R, Combs C, Tuveson DA, Vonderheide RH. Dynamics of the immune reaction to pancreatic cancer from inception to invasion. Cancer Res. Oct 1 2007;67(19):9518–9527. [PubMed: 17909062]
19. Roth S, Zamzow K, Gaida MM, et al. Evolution of the immune landscape during progression of pancreatic intraductal papillary mucinous neoplasms to invasive cancer. EBioMedicine. Apr 2020;54:102714. [PubMed: 32259711]

Synopsis:

The immune infiltrate of IPMN is primarily composed of T cells and macrophages. Regions of HGD appear to be enriched for macrophages and relatively deplete of T cells compared to regions of LGD.

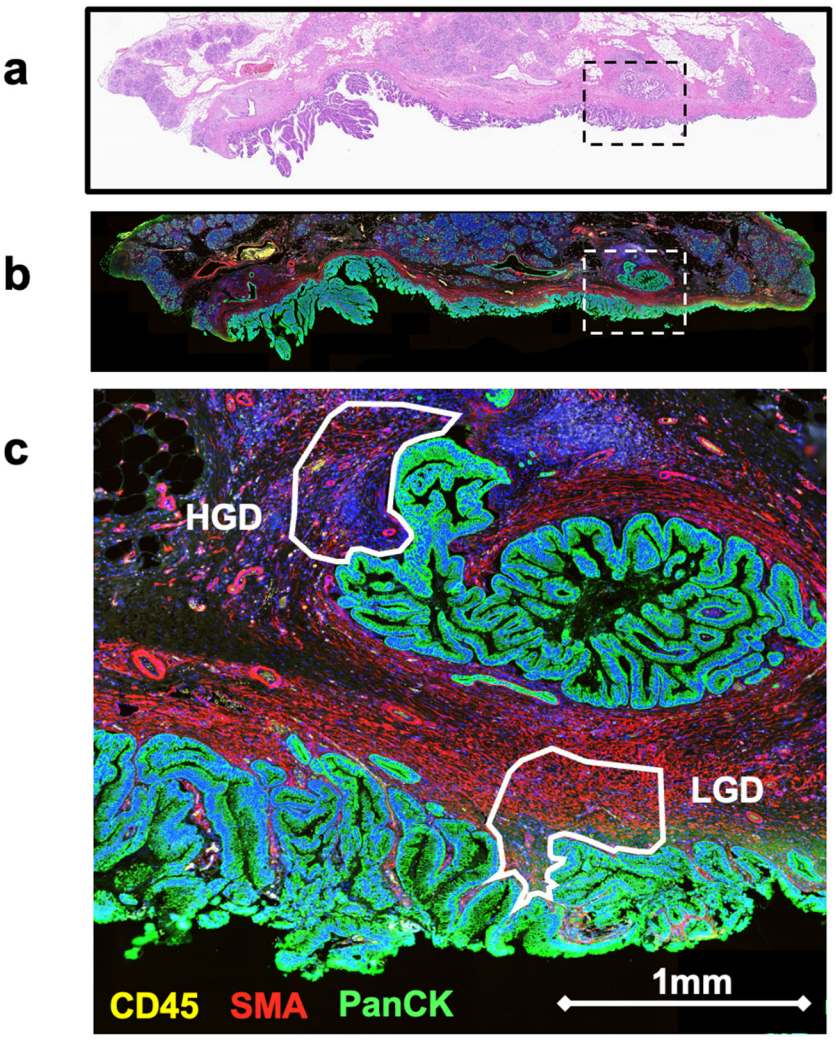

Figure 1:

Selection of ROIs within IPMN. A) A low power H&E of IPMN tissue containing regions of LGD and HGD. B) A low power spatial transcriptomics generated image with fluorescent staining DNA (blue), PanCK (green), CD45 (yellow), and SMA (red). The boxed region contains two ROIs seen in Figure 1c. C) A high power magnification of two stroma ROIs. ROIs are annotated according to the grade of dysplasia present within adjacent epithelium.

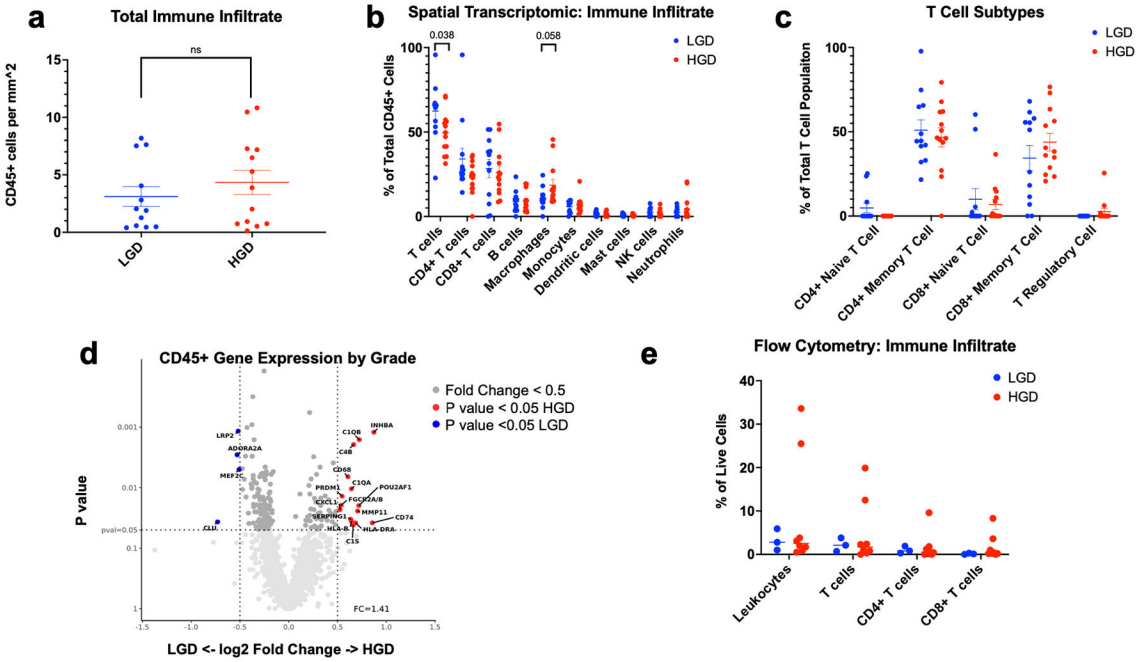

Figure 2:

Tumor Immune Infiltrating Lymphocytes by Grade of Dysplasia. A) The number of CD45+ cells per mm^2 by grade of dysplasia was measured by SpatialDecon. Mean and standard error of mean (SEM) are marked. A Mann-Whitney test found no statistical difference between LGD and HGD. B) The abundance of immune cell subtypes as a percentage of the total immune infiltrate within the IPMN stroma was determined and a Mann-Whitney test found total T cells to be significantly increased in LGD than HGD. C) The abundance of T cell subtypes as a percentage of total T cell was measured. There was no statistical difference between LGD and HGD. D) Differential gene expression between LGD and HGD. Volcano plots depict the fold change (log 2) and the p value (0.05) for each gene. Fold change represents read counts between LGD and HGD. E) Immune cell subtypes as a percentage of total CD45+ cells within single cell suspension of IPMN tissue was measured by flow cytometry. T cells were the most abundant cell type within the IPMN tissue. There was no statistical difference between by LGD and HGD by a Mann-Whitney test.

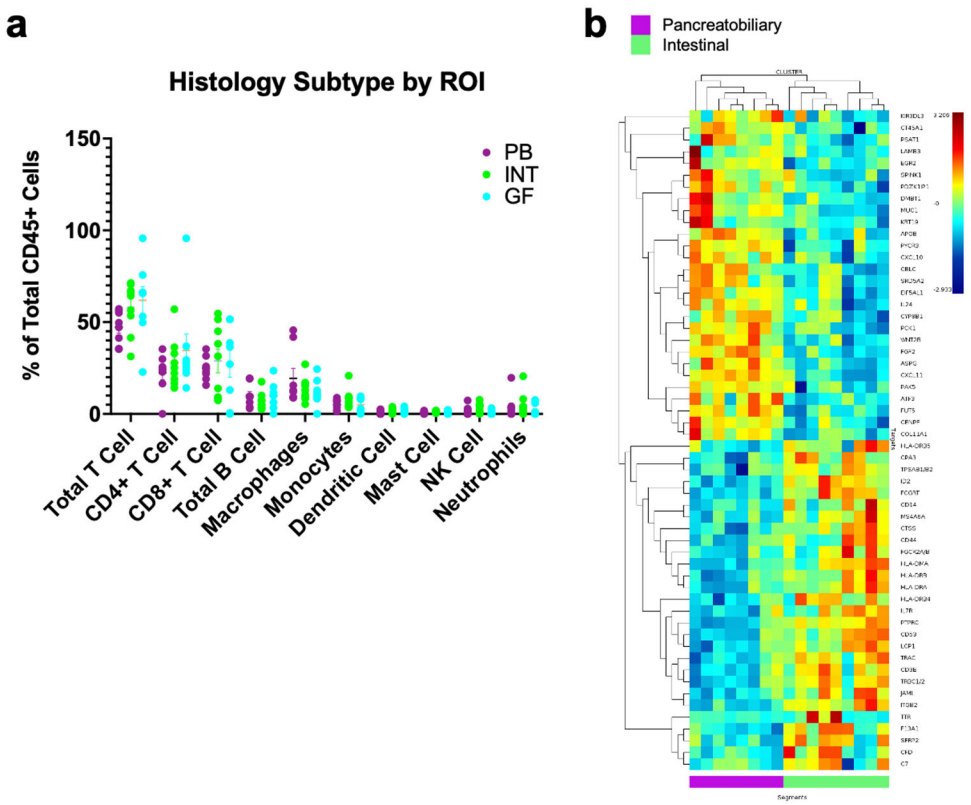

Figure 3:

Tumor Immune Infiltrating Lymphocytes by histology subtype (pancreatobiliary vs intestinal). A) The abundance of immune cell subtypes as a percentage of the total immune infiltrate within the IPMN stroma was determined by SpatialDecon. Mean and SEM are marked. There was a trend towards intestinal lesions having greater total T cell abundance than pancreatobiliary lesions. B) Heatmap and hierarchal clustering showing differential gene expression between pancreatobiliary and intestinal histology subtypes. Genes were selected for having a significant (P value <0.05) correlation and a 1.5 fold change between pancreatobiliary and intestinal subtype.

Table 1:

Patient characteristics in the spatial transcriptomics versus flow cytometry cohort.

	Spatial Transcriptomics	**Flow Cytometry**
	N = 12	**N = 11**
Median age: years (IQR)	70 (63-77)	71 (65-74)
Female Sex	5 (42%)	5 (45%)
Race		
Caucasian	8 (67%)	10 (91%)
Asian	3 (25%)	1 (9%)
Black	0 (0%)	0 (0%)
Unidentified	1 (8%)	0 (0%)
Operation		
Whipple	9 (75%)	5 (45%)
Distal Pancreatectomy	2 (17%)	5 (45%)
Other	1 (8%)	1 (9%)
Median Lesion Size, cm	5.2	3.8
Branch Type		
Main Branch	5 (42%)	4 (36%)
Side Branch	3 (25%)	4 (36%)
Mixed	4 (33%)	3 (27%)
Histology Subset		
Intestinal	6 (50%)	2 (18%)
Pancreatobiliary	6 (50%)	5 (45%)
Gastric	0 (0%)	4 (36%)
Cancer Present within Lesion	4 (33%)	5 (45%)
Cancer Stage if Applicable	IA (2), IIA (2)	IA (1), IB (1), IIA (1), IIB (2)
Median Follow up Length, months	27	24
Cancer Recurrence	2 (50%)	3 (60%)
Death	3 (25%)	0 (0%)